Hindawi
Advances in Condensed Matter Physics
Volume 2018, Article ID 6746023, 8 pages
https://doi.org/10.1155/2018/6746023

Research Article

Boson Peak and Superstructural Groups in Na_2O-B_2O_3 Glasses

Armenak A. Osipov and Leyla M. Osipova

Institute of Mineralogy of UB RAS, 456317, Miass, Russia

Correspondence should be addressed to Armenak A. Osipov; armik@mineralogy.ru

Received 20 August 2018; Revised 30 October 2018; Accepted 20 November 2018; Published 3 December 2018

Academic Editor: Luis L. Bonilla

Low-frequency Raman spectra of the sodium borate glasses with Na_2O content ranging from 0 to 30 mol% were measured and analyzed from the point of view of their structure in the intermediate range order. Our results show that there is a simple linear correlation between correlation length, l_c, and an average size, $<R>$, of the area of ordered arrangement of atoms, obtained via the distribution of the (super)structural units and their representative size. Six types of the areas of ordered arrangement of atoms were determined, being related to the presence of the $B_3O_3\varnothing_3$ boroxol rings, $B_3O_3\varnothing_4^-$ triborate rings, $B_5O_6\varnothing_4^-$ pentaborate groups, $B_8O_{10}\varnothing_6^{2-}$ tetraborate groups, $B_4O_5\varnothing_4^{2-}$ diborate groups, and $B_3O_6^{3-}$ cyclic metaborate anions in the sodium borate glasses. It was shown that the size of the areas of ordered arrangement of atoms can be determined from the simple geometric analysis of the crystallographic data on the superstructural units.

1. Introduction

It is accepted to distinguish two hierarchical structural levels in the structure of borate glasses. These glasses may be considered as an assembly of different boron-oxygen polyhedra at the level of the short range order (SRO) (the first hierarchical level). The polyhedra can be structurally characterized and identified in terms of the bond length and angles. Numerous studies of the local structure of borate glasses and crystals have shown that the boron atoms may be both three-fold and four-fold coordinated by oxygen. It is accepted, in turn, to classify oxygen atoms into two types: bridging oxygen atoms (BO), which form B-O-B bridging bonds belonging to two boron atoms simultaneously, and nonbridging oxygen atoms (NBO or terminal oxygen atoms), which do not form B-O-B bonds and belong only to one boron atom. Thus, five basic structural units are usually distinguished in borates according to the coordination number of the boron atoms and to the number of BOs and NBOs belonging to the given boron atom: $B\varnothing_3$ symmetric triangle ($\varnothing$ is BO), $[B\varnothing_4]^-$ borate tetrahedron, $B\varnothing_2O^-$ metaborate triangle, $B\varnothing O_2^{2-}$ pyroborate unit, and BO_3^{3-} orthoborate anion. All of these basic structural units can be identified experimentally, e.g., by NMR or vibrational spectroscopies, and to date, the local structure of borate glasses is well studied both qualitatively and quantitatively. It was established that an addition of alkali oxides to B_2O_3 leads, first of all, to transformation of $B\varnothing_3$ symmetric triangles into $[B\varnothing_4]^-$ tetrahedra and then to the formation of the structural units with NBOs. Thus, the $B\varnothing_3$ symmetric triangles and $[B\varnothing_4]^-$ tetrahedra are dominant structural units in structure of all alkali borate glasses with M_2O < 25-30 mol% (M = Li, Na, K, Rb and Cs). The concentration of the $[B\varnothing_4]^-$ units, N_4, does not depend (or slightly depends) on the type of alkali cation and N_4 as a function of mole fraction of alkali-metal oxide, x, follows $x/(1\text{-}x)$ equation in the indicated compositional range [1–3].

In [3–5], however, it was noted that the scale of the short range order does not reflect all the complexity of borate glasses, whose structure is characterized by the presence of the so-called superstructural units (boroxol rings, triborate rings, pentaborate groups, diborate groups, etc.) in the next hierarchical level (intermediate range order (IRO)). The superstructural units consist of well defined arrangements of basic structural units with no internal degrees of freedom in the form of variable bond and/or torsion angles [6–8]. A rigidly defined atomic position in these groups allows interpreting the superstructural units as IRO structures of borate glasses. Investigation of distribution of the superstructural

units directly, e.g., with using vibrational spectroscopy or NMR technique, is often problematic due to the ambiguity in identification of these groups [4, 5]. In turn, this leads to the problems of measurement of their concentration in glasses with various compositions. Therefore, experimental data on distribution of superstructural units are typically limited by area of their existence and by general tendencies of variation in their concentrations with change in modifier oxide content [9–11]. This fact does not allow to perform a depth study of the dependence of fraction of superstructural units on a glass composition and type of alkali cation.

Investigation of the low-frequency light scattering (Boson peak) plays important role for study of a glass structure. Today, there is no common opinion on the origin of the Boson peak and this problem is open for discussion. One idea is that the Boson peak is caused from vibrational excitations made up of acoustic phonons (most likely shear or transverse phonons) which scatter strongly from elastic inhomogeneities in the glass structure. The scattering leads to a drastic decrease of the mean free path of vibrations and can increase the vibrational density of states in a certain frequency range. The phonon localization may be viewed in terms of the Ioffe–Regel criteria ($\lambda \sim l$, where λ is phonon wavelength and l is mean free phonon path). These criteria allow to define the correlation length, l_c, through the Boson peak frequency, ω_{BP}, and the sound velocity, v_s [12]:

$$l_c \approx \frac{v_s}{\omega_{BP}} \quad (1)$$

The study of the composition and concentration dependence of the low-frequency light scattering spectra of the borate glasses [13, 14] has shown that both the type of the alkali metal cation and the concentration of modifier oxide strongly affect the spectral properties of the Boson peak (intensity and Boson peak position) (see, e.g., Fig. 18 in ref. [13] or Fig. 7 in ref. [14]) and, hence, the dynamic correlation length l_c. This clearly indicates that IRO structures of various alkali borate glasses are essentially different even if their local structure is qualitatively and quantitatively similar.

Significant progress in understanding of the structure of borate glasses at the level of superstructural units was achieved in the framework of the thermodynamic approach to modeling the properties and structure of the oxide glasses [15]. It was shown that the chemical structure of the lithium and sodium borate glasses and, therefore, the distribution of the superstructural units in these glasses, differ significantly (see, e.g., Fig. 19 in ref. [16] or Fig. 23 and 30 in ref. [8]). At the same time, their local structure is identical at $0 \le x \le$ 25-30 mol%. Thus, the results of the thermodynamic modeling also testify that the type of alkali cation strongly affects the IRO structures of alkali borate glasses.

The aim of our study is studying of an interrelationship between dynamic correlation length, l_c, and distribution of the superstructural units in sodium borate glasses.

2. Materials and Methods

The glasses with composition $x\mathrm{Na_2O}$-(100-x)$\mathrm{B_2O_3}$ (where x is the molar concentration of $\mathrm{Na_2O}$ ranging from 0 to 30 mol%) were prepared by the normal melt quenching method using $\mathrm{Na_2CO_3}$ and $\mathrm{H_3BO_3}$ as sources of sodium oxide and boron trioxide, respectively. The initial reagents were thoroughly mixed in the required ratios and placed in a platinum crucible (Pt). The batch (10 g) in a Pt crucible was placed into electrical furnace, where the temperature was gradually increased up to ~750-1000°C (depending on a glass composition). The fusion was carried out at the given temperatures for 2 hours, whereupon the melting was continued at 1100-1150°C for another one hour. Then, the clear and bubble free liquid was poured into a special steel mould preheated to the temperature close to the glass-transition temperature, T_g, (below 5-10°C than T_g) to obtain the glassy parallelepiped (7 × 7 × 10 mm, approximately). All glassy samples were annealed at temperature close to T_g for 3 hours. Two samples were prepared for each composition: one of them was used for the measurement of the low-frequency light scattering spectra and the other was used for determination of density (ρ).

The density of each annealed glass sample was measured using Archimedes principle at room temperature using kerosene as a worked liquid. The density was calculated using the formula

$$\rho = \frac{W_A}{W_A - W_B}\rho_B \quad (2)$$

where W_A and W_B are the weights of the sample in air and in kerosene, respectively, and ρ_B is the density of kerosene. The samples were weighted using an electronic digital balance (KERN ALS120-4) of uncertainty ± 0.0001 g.

The low-frequency Raman spectra were measured at a 90° scattering geometry using a double grating DFS-24 monochromator. Solid-state laser (LTI-701) with a wavelength of 532 nm (average power is 500 mW) was used as excitation source of spectra. An uncooled FEU-79 photomultiplier, operating in photon counting regime, was employed to collect the low-frequency Raman spectra. The spectral width of the slit was equal to 2 $\mathrm{cm^{-1}}$ in all experiments.

3. Results and Discussion

Nominal glass compositions (in mol%), their designations as well as the velocity of transverse ultrasonic waves, v_t, are presented in Table 1. In addition, the "real" composition of the glasses obtained on the basis of comparison of the density of studied glasses with the data from the literature [17–20] (see Figure 1) is shown in the third column of the Table 1. One can see that the difference between nominal and "real" glass compositions is in the reasonable limits and is less than 0.5 mol%. At the same time, our data are in a good agreement with those published in the literature. The "real" glass composition, therefore, will be used in further discussion.

The examples of the low-frequency Raman spectra for a series of sodium borate glasses are shown in Figure 2. Two main tendencies are observed with variation in modifier oxide content: (i) shift of the Boson peak maximum toward the higher wavenumbers and (ii) decrease in its intensity

Table 1: Samples designation, nominal composition, and "real" composition of xNa$_2$O-(100-x)B$_2$O$_3$ (x is given in mol%) glasses as well as the velocity of transverse ultrasonic waves, v_t. The velocities of transverse ultrasonic waves, v_t, were obtained via the method of the piecewise-linear approximation of the corresponding data published in ref. [17].

Sample designation	Nominal composition [mole%]	«Real» composition [mole%]	v_t [ms^{-1}]
NB1	0	0	1900
NB2	2.5	2.5	2080
NB3	5	5	2240
NB4	7.5	7.1	2365
NB5	10	9.5	2478
NB6	12.5	12.5	2595
NB7	15	14.5	2663
NB8	17.5	17.1	2743
NB9	20	20	2842
NB10	22.5	22.2	2928
NB11	25	25	3045
NB12	27.5	27.5	2133
NB13	30	30	3190

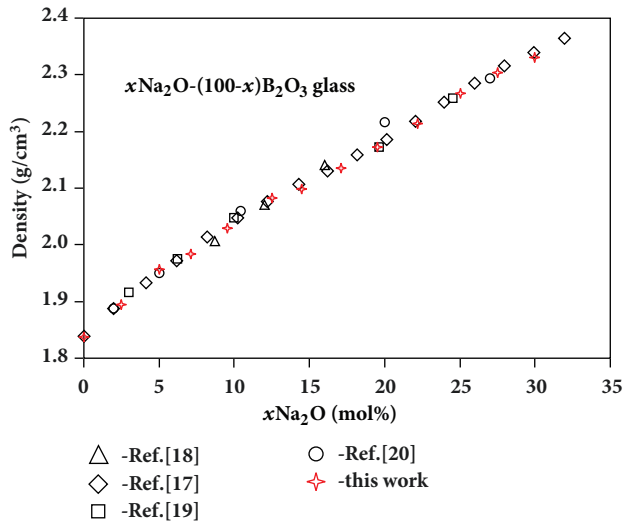

Figure 1: Density of the Na$_2$O-B$_2$O$_3$ glasses as a function of Na$_2$O content.

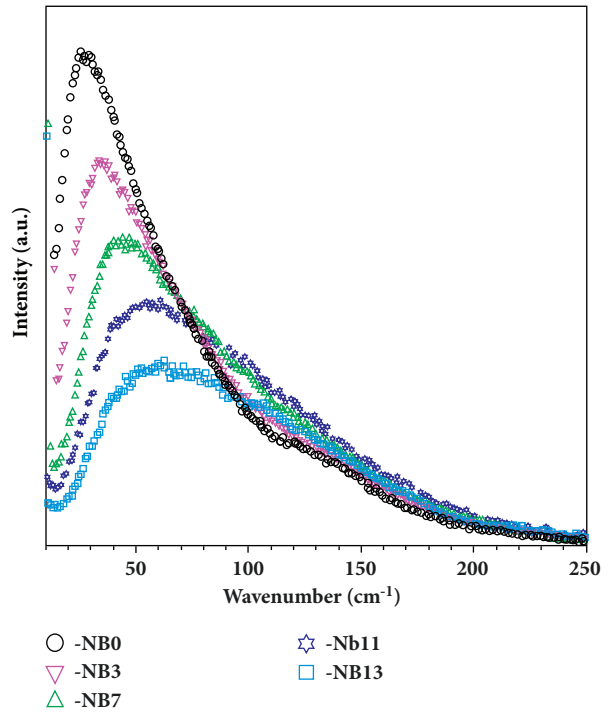

Figure 2: Examples of the low-frequency Raman scattering spectra of Na$_2$O-B$_2$O$_3$ glasses.

with an increase in Na$_2$O content. Similar behavior was found in ref. [21]. Furthermore, a comparison of the Boson peak position showed that our results are in a reasonable accordance (within the experimental errors) with the data published in ref. [21] (see Figure 3). Composition dependence of the dynamic correlation length l_c calculated according to the Eq. (1) is shown in Figure 4. The $l_c(x)$ function was obtained using velocity of transverse ultrasonic waves, v_t, presented in Table 1. As seen from this figure, an increase in sodium oxide content leads to the systematic decrease in the dynamic correlation length l_c from ~ 2.3 nm (g-B$_2$O$_3$) to ~ 1.7-1.8 nm (NB13 glass).

As shown in refs. [13, 21], some characteristic length, which we will denote here as L (L is not the same that l_c), can be determined through the analysis of the low-frequency Raman scattering spectra. The L is the "short correlation length" according to ref. [13] or it is the intermolecular distance between the centers of interacting groups according to ref. [21]. Both these works show that L systematically changes with the change in the glass composition and give L ~ 7.5-8 Å for g-B$_2$O$_3$. It is reasonable to consider a B$_2$O$_3$ structure in order to understand the meaning of this length.

It is known that the glassy B$_2$O$_3$ consists of B$\varnothing_3$ planar triangles. A major portion of these triangles (up to ~80%

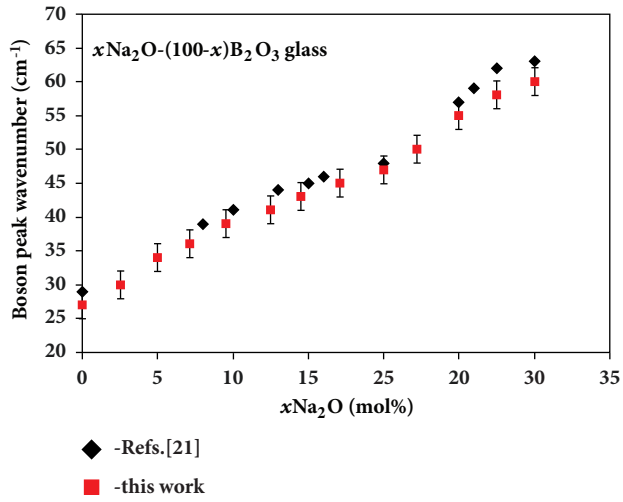

Figure 3: Boson peak wavernumber versus glass composition.

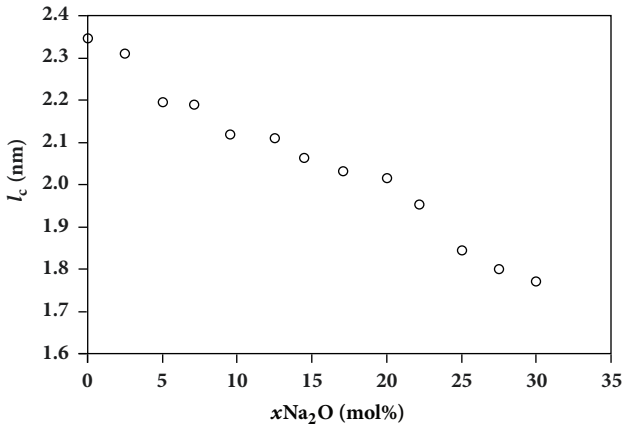

Figure 4: Composition dependence of the correlation length l_c.

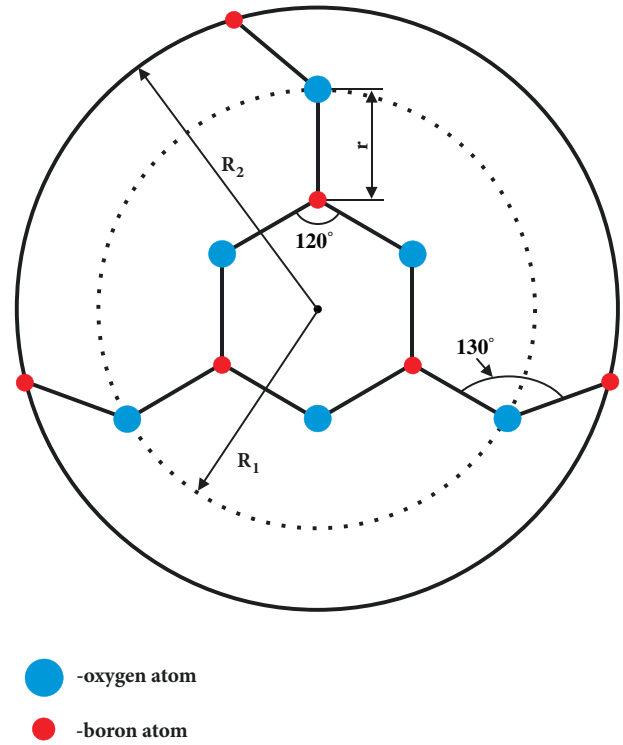

Figure 5: Schematic illustration of the $B_3O_3\varnothing_3$ boroxol ring.

according to refs. [7, 22, 23]) is associated into the so-called $B_3O_3\varnothing_3$ boroxol rings, which contain three $B\varnothing_3$ units. The $B_3O_3\varnothing_3$ boroxol ring is a sole type of the superstructural units existing in the g-B_2O_3. Schematic illustration of the $B_3O_3\varnothing_3$ boroxol ring is shown in Figure 5. This figure is useful when considering the correlation between the structure of pure g-B_2O_3 and some characteristic length L. For the fixed length of the B-O bonds (r = 1.365 Å [7]) and O-B-O angles (~120°) within the $B\varnothing_3$ units, a diameter of the boroxol ring ($2R_1 = 4r$) will be equal to ~5.5 Å. This value is less than characteristic length, L ~7.5-8 Å [13, 21], for the glassy B_2O_3. Hence it follows that the ordered arrangement of atoms in g-B_2O_3 is not limited by the size of the boroxol ring, but it noticeably in excess of its diameter. It was suggested [21] that the ordered arrangement of atoms in g-B_2O_3 may extend outside the boroxol ring, down to the nearest boron atoms, which are not included into the ring. In the given case, the 7.5 Å corresponds to the $2R_2$ distance (see Figure 5). This distance is obtained if the B-O-B external angle, which is not included into the boroxol ring, is equal to 130°. A good agreement between experimental [13, 21] and theoretical (obtained via the simple geometric analysis) L values allows us to assume that the B-O-B angle is not changed completely at random. It is evident from Figure 5 that the characteristic length in the glassy B_2O_3 can be interpreted as a distance between the centers of two nearest-neighbor boroxol rings. Such interpretation is in accordance with assumption that the $B_3O_3\varnothing_3$ boroxol rings are not linked to each other completely at random in structure of g-B_2O_3 [13]. On the other hand, the geometric analysis allows interpreting the L length as a distance, characterizing the size of the area of ordered arrangement of atoms in g-B_2O_3. From this point of view, it is obvious that the L distance will change at an increase in concentration of modifier oxide; i.e., L is a function of the glass composition.

As mentioned in "Introduction", addition of the sodium oxide leads to the changes in the SRO and IRO structures in sodium borate glasses. The changes of SRO structures are related to the increase in coordination number of boron atoms from 3 to 4. In turn, the formation of the $[B\varnothing_4]^-$ tetrahedra is reflected in IRO structures: the boroxol rings are transformed into the other superstructural units with $[B\varnothing_4]^-$ tetrahedra. According to the results of the thermodynamic modeling [5, 24], an increase in concentration of Na_2O, first, leads to appearance of the $B_3O_3\varnothing_4^-$ triborate rings and $B_5O_6\varnothing_4^-$ pentaborate groups, simultaneously, and then, the $B_4O_5\varnothing_4^{2-}$ diborate groups and $B_3O_6^{3-}$ cyclic metaborate anions start to appear in the structure of studied glasses. An increase in the fraction of $B_3O_3\varnothing_4^-$ triborate and $B_5O_6\varnothing_4^-$ pentaborate groups is accompanied by a decrease in concentration of the $B_3O_3\varnothing_3$ boroxol rings. In turn, an

increase in concentration of $B_4O_5\varnothing_4^{2-}$ diborate and $B_3O_6^{3-}$ metaborate groups is accompanied by a decrease in fraction of pentaborate and triborate groups (see Fig. 5 in ref. [24]).

By the definition given in the "Introduction", each of the above mentioned superstructural units is the area of ordered arrangement of atoms. Thus, for the glass with any given composition, an average size, <*R*>, of the area of ordered arrangement of atoms can be expressed as follows:

$$\langle R\rangle(x) = \sum N_i(x)\, R_i \tag{3}$$

Here, N_i and R_i are the concentration and representative size of the area of the ordered arrangement of atoms, respectively, near or within the limits of the superstructural group. Subscript i indicates the type of superstructural units: i = B (boroxol ring), T (triborate ring), P (pentaborate group), D (diborate group), and M (metaborate ring). All necessary data on the concentration of the superstructural units can be readily obtained from refs. [4, 24]. The compositional dependencies of various superstructural units within the range under consideration are shown in Figure 6. One can see that, to calculate the average size <*R*>, four representative sizes (for the $B_3O_3\varnothing_4^-$ triborate ring, $B_5O_6\varnothing_4^-$ pentaborate group, $B_4O_5\varnothing_4^{2-}$ diborate group, and $B_3O_6^{3-}$ cyclic metaborate anion) should be determined in the studied composition range ($0 \le x \le 30$ mol%).

It is evident that the linear size of the ring-type superstructural units, such as triborate and metaborate rings, at the first approximation, can be considered to be equal to the diameter of circle circumscribed around of the boroxol ring, i.e., $R_T = R_M = R_B = 2R_1 \sim 5.5$ Å (see Figure 5). The strict location of atoms in the pentaborate group (Figure 7), as shown in ref. [25], leads to the fact that this group can be unambiguously described via seven independent parameters: four lengths of B-O bonds and three O-B-O angles (see Table 6 in ref. [25]). Based on these data, one can estimate the linear sizes of the pentaborate group. As seen from Figure 7, the pentaborate group has a maximum size along X-axis ($R_X^P = 2R_1^P$), whereas its sizes along Y and Z axes will be equal ($R_Y^P = R_Z^P$) and less than $R_X^P = 2R_1^P$ (for the orientation presented in the figure). Taking into account that the characteristic size of the ring-type superstructural units is the diameter of circle circumscribed around of such groups, it was assumed that, among two specific sizes of the pentaborate group, R_X^P and $R_Y^P = R_Z^P$, the maximum size should be used for calculation of the <*R*>(x) function according to Eq. (3). Thus, using the data published in ref. [25], we have found that $R_P = R_X^P = 2R_1^P \sim 5.84$ Å.

Diborate group (Figure 8) consists of two $B\varnothing_3$ symmetric triangles and two $[B\varnothing_4]^-$ tetrahedra. The fixed position of atoms in this group is described by nine independent parameters: five lengths of B-O bonds and four O-B-O/B-O-B angles [25, 26]. Figure 8 shows that this group can be described by three linear sizes, R_X^D, R_Y^D and R_Z^D (linear size along Z-axis is not shown), and R_X^D size, obviously, is a maximum size. We have found that the linear size of the diborate group along X-axis, R_X^D, is equal to ~5.7 Å, based on the data presented in Table 7 in ref. [25]. Therefore, the

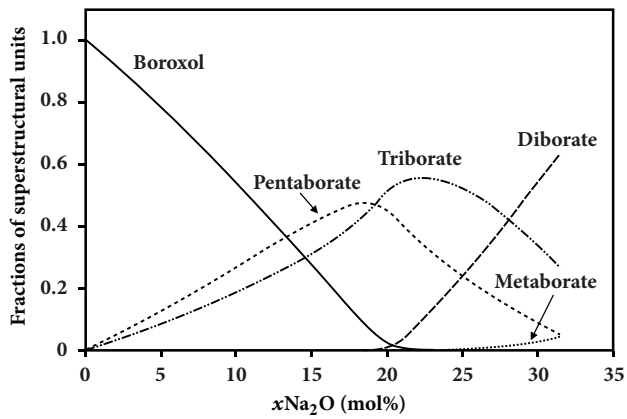

FIGURE 6: Distribution of the superstructural groups in Na_2O-B_2O_3 glasses.

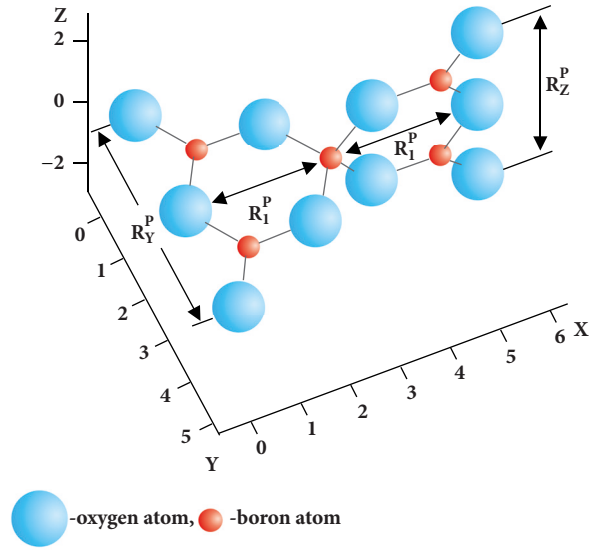

FIGURE 7: Schematic illustration of the $B_5O_6\varnothing_4^-$ pentaborate group.

representative size of the area of ordered arrangement of atoms within the limit of diborate group, R_D, was accepted to be 5.7 Å.

Thus, we have all necessary data (concentrations of superstructural units (Figure 6) and representative sizes of the areas of ordered arrangement of atoms: R_B = 7.5 Å, R_P = 5.84 Å, R_D = 5.7 Å and $R_T = R_M$ = 5.5 Å) to calculate the average size <*R*>, according to Eq. (3). The results of calculation are shown in Figure 9 (black dotted line). One can see that the theoretic curve is changed monotonously only in the limited composition ranges ($0 \le x \le 20$ mol%) and it remains practically unchanged with further increasing in Na_2O content. Therefore, a simple linear correlation between $l_c(x)$ and <*R*>(x) values is observed also in only the limited composition range ($x \le$ 15-20 mol%) and strong deviation from the linear behavior is observed at higher concentration of sodium oxide (see Figure 10(a)). This result can be

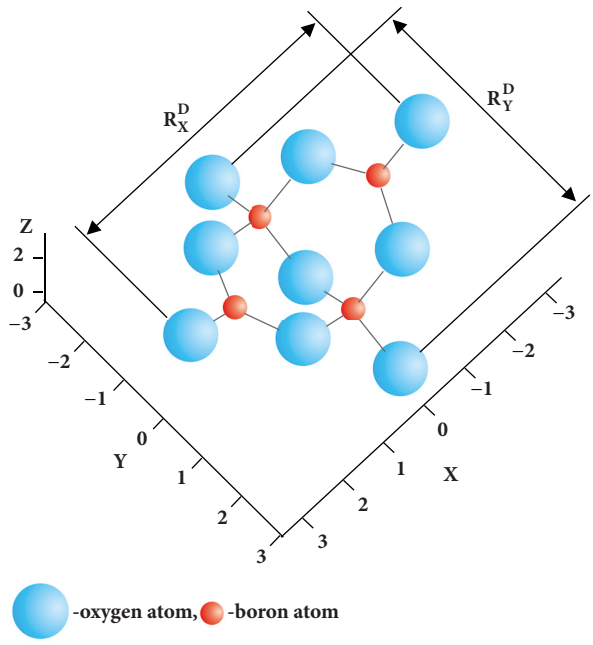

FIGURE 8: Schematic illustration of the $B_4O_5\varnothing_4^{2-}$ diborate group.

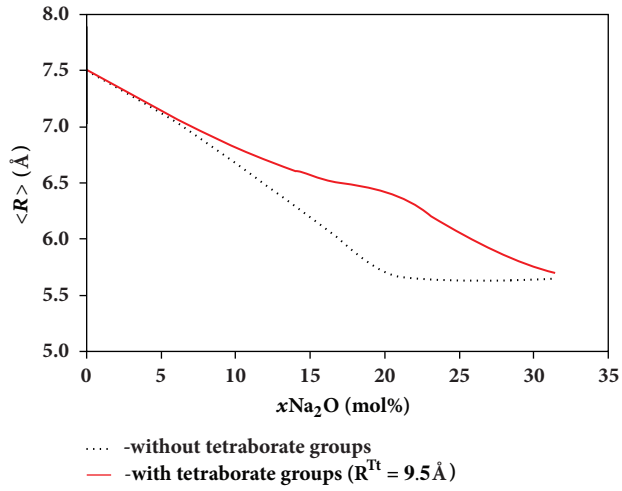

FIGURE 9: Composition dependence of the average size <*R*> of the area of ordered arrangement of atoms in sodium borate glasses. Black dotted and red solid lines are the results of calculations according to Eq. (3) without and with regard to the tetraborate group, respectively.

explained if we assume that some type of the area of ordered arrangement of atoms was ignored in our calculations.

There are numerous works [9, 11, 14, 27–31] where it was shown that $B_8O_{10}\varnothing_6^{2-}$ tetraborate groups are also present in structure of the sodium borate glasses in addition to those presented in Figure 6. The $B_8O_{10}\varnothing_6^{2-}$ tetraborate group is not a superstructural unit [8, 16], because it consists of $B_5O_6\varnothing_4^-$ pentaborate group and $B_3O_3\varnothing_4^-$ triborate ring, which are connected to each other by bridging oxygen atom (see Figure 11). For this reason, the tetraborate groups are absent in the distribution of the superstructural units [24] and, hence, they were ignored initially. Nevertheless, the $B_8O_{10}\varnothing_6^{2-}$ group represents the local area of the ordered arrangement of atoms and, hence, it should be taken into account for calculation of the $<R>(x)$ function according to Eq. (3). Unfortunately, no unambiguous information is known on the concentration of tetraborate groups in structure of the sodium borate glasses. For this reason, at the first approximation, the concentration of the tetraborate group was defined as a product of concentrations of triborate and pentaborate groups. New distribution of the IRO structures obtained under this assumption is shown in Figure 12.

The linear size of the $B_8O_{10}\varnothing_6^{2-}$ tetraborate group may be estimated on the basis of new distribution of IRO structures: R_{Tt} size can be chosen so that the correlation factor, R^2, between l_c, and <*R*>, will be more than any preassigned value ($R^2 \geq 0.98$ in this work). It was found that a good correlation between correlation length, l_c, and average size, <*R*>, is observed at R_{Tt} ~9.5-9.6 Å. It is evident that R_{Tt} value may match to the linear size of the tetraborate group along X-axis for the orientation presented in Figure 11. New $<R>(x)$ dependence is shown in Figure 9 by red solid line.

On the other hand, one can estimate this size based on the data about the structure of crystalline sodium tetraborate [32]. Such estimation provides the maximum linear size of the tetraborate group of 10 Å, approximately. This result is consistent with previously found R_{Tt} of ~9.5-9.6 Å. Thus, the inclusion in consideration of the $B_8O_{10}\varnothing_6^{2-}$ tetraborate group leads to the fact that between $l_c(x)$ and $<R>(x)$ dependencies a simple linear correlation is observed (see Figure 10(b)).

4. Conclusions

The low-frequency light-scattering spectra of a series of sodium borate glasses with sodium oxide content ranging from 0 to 30 mol% were measured. The spectra were analyzed to find a compositional dependence of the correlation length, $l_c(x)$, and its interrelation with the IRO structures in the studied glasses. The correlation length l_c was determined according with Ioffe–Regel criteria and it decreases systematically with the increase in Na_2O content. In turn, the average size, <*R*>, of the area of ordered arrangement of atoms was determined via the data of the thermodynamic modeling of the distribution of the superstructural units and the geometric analysis of the superstructural units. Six types of areas of the ordered arrangement of atoms were determined. Each of them was related to the presence of the $B_3O_3\varnothing_3$ boroxol rings, $B_3O_3\varnothing_4^-$ triborate rings, $B_5O_6\varnothing_4^-$ pentaborate groups, $B_8O_{10}\varnothing_6^{2-}$ tetraborate groups, $B_4O_5\varnothing_4^{2-}$ diborate groups, and $B_3O_6^{3-}$ cyclic metaborate anions. For the ring-type groups, such as boroxol ring, triborate ring, and cyclic metaborate anion, the representative size can be expressed through the diameter of the circle circumscribed around them. If the shape of the large grouping significantly differs from the ring (e.g., pentaborate group, tetraborate group, and diborate group), then the representative size of the area of the ordered arrangement of atoms is

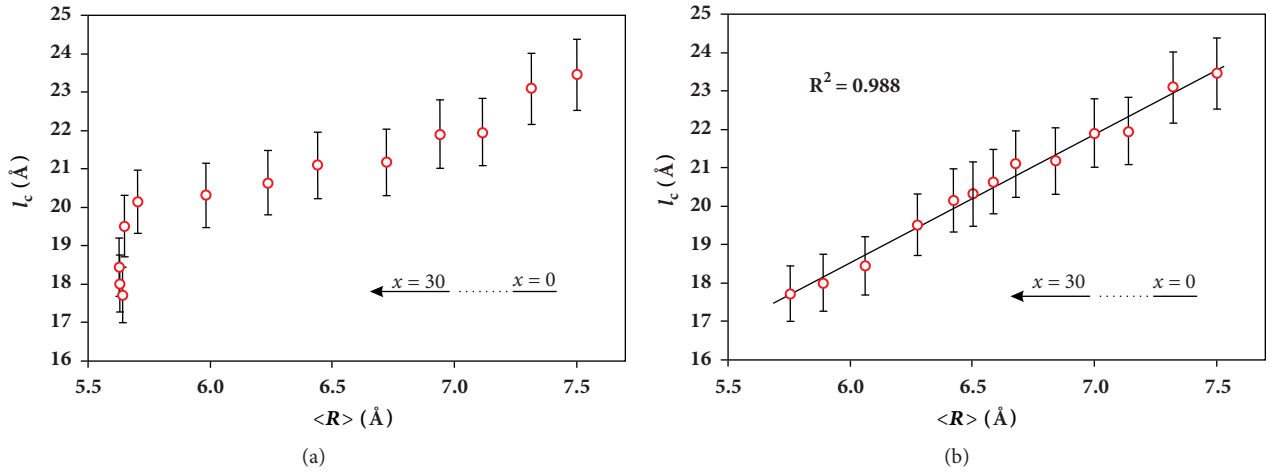

FIGURE 10: Correlations between $l_c(x)$ and $<R>(x)$ functions for the sodium borate glasses without (a) and with regard to (b) the tetraborate group.

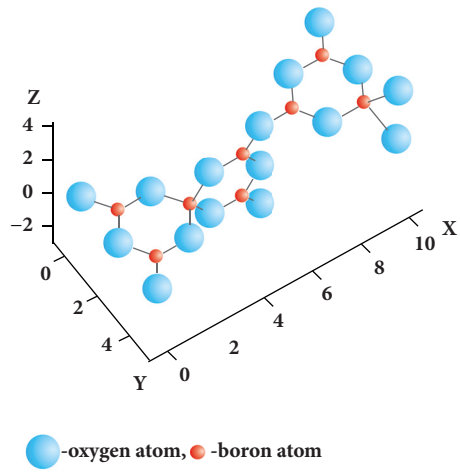

FIGURE 11: Schematic illustration of the $B_8O_{10}\varnitrogen_6^{2-}$ tetraborate group.

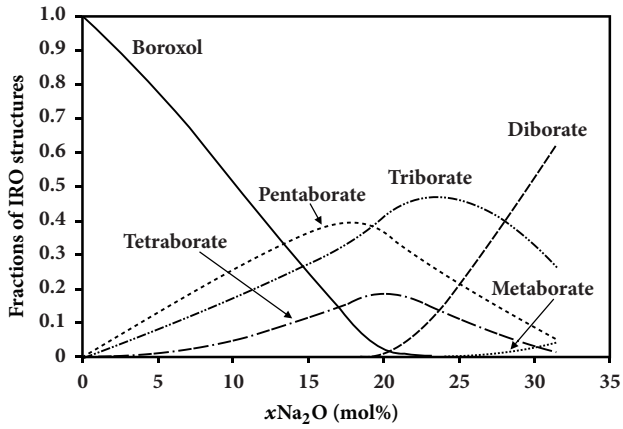

FIGURE 12: Distribution of the IRO structures in Na_2O-B_2O_3 glasses.

determined by the maximum linear size of such groups. In case of the pure g-B_2O_3, the area of the ordered arrangement of atoms (7.5 Å) exceeds the diameter of the boroxol ring that indicates the extension of the ordered arrangement of atoms beyond the ring. The representative size of the area of the ordered arrangement of atoms does not exceed the maximum linear size of the corresponding group in all other cases (5.5, 5.84, 9.4-9.5, 5.7, and 5.5 Å for the triborate ring, pentaborate group, tetraborate group, diborate group, and metaborate ring, resp.). It was found that there is a simple linear correlation between the correlation length, l_c, and the average size, $<R>$, of the area of ordered arrangement of atoms.

Data Availability

The data (density, sound velocity, low-frequency Raman spectra, and distribution of the superstructural groups) used to support the findings of this study are included within the article.

Conflicts of Interest

The authors declare that there are no conflicts of interest regarding the publication of this paper.

Acknowledgments

This work was supported by state contract [AAAA-A16-116012510127-9] and state task no. 11.9643.2017/BCh of the Ministry of Education and Science of Russia.

References

[1] V. K. Michaelis, P. M. Aguiar, and S. Kroeker, "Probing alkali coordination environments in alkali borate glasses by multinuclear magnetic resonance," *Journal of Non-Crystalline Solids*, vol. 353, no. 26, pp. 2582–2590, 2007.

[2] W. J. Clarida, J. R. Berryman, M. Affatigato et al., "Dependence of N4 upon alkali modifier in binary borate glasses," *Physics and Chemistry of Glasses*, vol. 44, pp. 215–217, 2003.

[3] S. Kroeker, P. Aguiar, A. Cerquiera et al., "Alkali dependence of tetrahedral boron in alkali borate glasses," *Physics and Chemistry of Glasses: European Journal of Glass Science and Technology Part B*, vol. 47, pp. 393–396, 2006.

[4] N. M. Vedishcheva and A. C. Wright, "Chemical structure of oxide glasses: A concept for establishing structure-property relationships," in *Glass: Selected properties and crystallization*, J. W. P. Schmelzer, Ed., pp. 269–299, De Gruyter, Berlin/Boston, 2014.

[5] A. C. Wright and N. M. Vedishcheva, "Superstructural unit species in vitreous and crystalline alkali, alkaline earth and related borates," *Physics and Chemistry of Glasses: European Journal of Glass Science and Technology Part B*, vol. 54, pp. 147–156, 2013.

[6] A. C. Wright, B. A. Shakhmatkin, and N. M. Vedishcheva, "The chemical structure of oxide glasses: A concept consistent with neutron scattering studies?" *Glass Physics and Chemistry*, vol. 27, no. 2, pp. 97–113, 2001.

[7] A. C. Wright, R. N. Sinclair, D. I. Grimley et al., "Borate glasses, superstructural units and random network theory," *Physics and Chemistry of Glasses*, vol. 22, pp. 268–278, 1996.

[8] A. C. Wright, "Borate structures: crystalline and vitreous," *Physics and Chemistry of Glasses: European Journal of Glass Science and Technology Part B*, vol. 51, pp. 1–39, 2010.

[9] B. N. Meera and J. Ramakrishna, "Raman spectral studies of borate glasses," *Journal of Non-Crystalline Solids*, vol. 159, no. 1-2, pp. 1–21, 1993.

[10] E. I. Kamitsos and M. A. Karakassides, "Structural studies of binary and pseudo binary sodium borate glasses of high sodium content," *Physics and Chemistry of Glasses: European Journal of Glass Science and Technology Part B*, vol. 30, no. 1, pp. 19–26, 1989.

[11] W. L. Konijnendijk and J. M. Stevels, "The structure of borate glasses studied by Raman scattering," *Journal of Non-Crystalline Solids*, vol. 18, no. 3, pp. 307–331, 1975.

[12] J. Schroeder, W. Wu, J. L. Apkarian, M. Lee, L.-G. Hwa, and C. T. Moynihan, "Raman scattering and Boson peaks in glasses: Temperature and pressure effects," *Journal of Non-Crystalline Solids*, vol. 349, no. 1-3, pp. 88–97, 2004.

[13] J. Lorösch, M. Couzi, J. Pelous, R. Vacher, and A. Levasseur, "Brillouin and raman scattering study of borate glasses," *Journal of Non-Crystalline Solids*, vol. 69, no. 1, pp. 1–25, 1984.

[14] B. P. Dwivedi and B. N. Khanna, "Cation dependence of raman scattering in alkali borate glasses," *Journal of Physics and Chemistry of Solids*, vol. 56, no. 1, pp. 39–49, 1995.

[15] B. A. Shakhmatkin and N. M. Vedishcheva, "A thermodynamic approach to the modeling of physical properties of oxide glasses," *Glass Physics and Chemistry*, vol. 24, no. 3, pp. 229–236, 1998.

[16] A. C. Wright, G. Dalba, F. Rocca, and N. M. Vedishcheva, "Borate versus silicate glasses: why are they so different?" *Physics and Chemistry of Glasses: European Journal of Glass Science and Technology Part B*, vol. 51, pp. 233–265, 2010.

[17] M. Kodama and S. Kojima, "Velocity of sound in and elastic properties of alkali metal borate glasses," *Physics and Chemistry of Glasses: European Journal of Glass Science and Technology Part B*, vol. 55, no. 1, pp. 1–12, 2014.

[18] E. Ratai, M. Janssen, and H. Eckert, "Spatial distributions and chemical environments of cations in single- and mixed alkali borate glasses: Evidence from solid state NMR," *Solid State Ionics*, vol. 105, no. 1-4, pp. 25–37, 1998.

[19] V. Mazurin, M. V. Strel'tsina, and T. P. Shvaiko-Shvaikovskaya, *Handbook on the properties of glasses and glass-forming melts*, vol. 4, Nauka, Leningrad, Russia, 1980.

[20] N. S. Abd El-Aal, "Study on ultrasonic velocity and elastic properties of γ-radiated borate glasses," *Bulgarian Journal of Physics*, vol. 28, pp. 275–288, 2001.

[21] A. V. Baranov, T. S. Perova, V. I. Petrov, J. K. Vij, and O. F. Nielsen, "Nature of the boson peak in Raman spectra of sodium borate glass systems: Influence of structural and chemical fluctuations and intermolecular interactions," *Journal of Raman Spectroscopy*, vol. 31, no. 8-9, pp. 819–825, 2000.

[22] G. E. Jr. Jellison, L. W. Panek, P. J. Bray, and G. B. Jr. Rouse, "Determination of structure and bonding in vitreous B_2O_3 by means of ^{10}B and ^{11}B and ^{17}O NMR," *The Journal of Chemical Physics*, vol. 66, pp. 802–812, 1977.

[23] A. C. Hannon, D. I. Grimley, R. A. Hulme, A. C. Wright, and R. N. Sinclair, "Boroxol groups in vitreous boron oxide: new evidence from neutron diffraction and inelastic neutron scattering studies," *Journal of Non-Crystalline Solids*, vol. 177, no. C, pp. 299–316, 1994.

[24] N. M. Vedishcheva, I. G. Polyakova, and A. C. Wright, "Short and intermediate range order in sodium borosilicate glasses: a quantitative thermodynamic approach," *Physics and Chemistry of Glasses: European Journal of Glass Science and Technology Part B*, vol. 55, pp. 225–236, 2014.

[25] A. C. Wright, J. L. Shaw, R. N. Sinclair, N. M. Vedishcheva, B. A. Shakhmatkin, and C. R. Scales, "The use of crystallographic data in interpreting the correlation function for complex glasses," *Journal of Non-Crystalline Solids*, vol. 345-346, pp. 24–33, 2004.

[26] A. C. Wright, R. N. Sinclair, C. E. Stone et al., "A neutron diffraction study of $2M_2O.5B_2O_3$ (M = Li, Na, K, Rb, Cs & Ag) and $2MO.5B_2O_3$ (M = Ca & Ba)," *Physics and Chemistry of Glasses: European Journal of Glass Science and Technology Part B*, vol. 53, pp. 191–204, 2012.

[27] P. J. Bray, S. A. Feller, G. E. Jellison Jr., and Y. H. Yun, "B10 NMR studies of the structure of borate glasses," *Journal of Non-Crystalline Solids*, vol. 38-39, no. 1, pp. 93–98, 1980.

[28] G. E. Jellison Jr. and P. J. Bray, "A structural interpretation of B10 and B11 NMR spectra in sodium borate glasses," *Journal of Non-Crystalline Solids*, vol. 29, no. 2, pp. 187–206, 1978.

[29] J. Krogh-Moe, "Structural interpretation of melting point depression in the sodium borate system," *Physics and Chemistry of Glasses*, vol. 3, pp. 101–110, 1962.

[30] J. Krogh-Moe, "On the structure of boron oxide and alkali borate glasses," *Physics and Chemistry of Glasses*, vol. 1, pp. 26–31, 1960.

[31] J. Krogh-Moe, "Interpretation of the infra-red spectra of boron oxide and alkali borate glasses," *Physics and Chemistry of Glasses: European Journal of Glass Science and Technology Part B*, vol. 6, pp. 46–54, 1965.

[32] A. Hyman, A. Perloff, F. Mauer, and S. Block, "The crystal structure of sodium tetraborate," *Acta Crystallographica*, vol. 22, no. 6, pp. 815–821.